

***Arabidopsis* SOMATIC EMBRYOGENESIS RECEPTOR KINASES1 and 2 Are Essential for Tapetum Development and Microspore Maturation**

Jean Colcombet, Aurélien Boisson-Dernier, Roc Ros-Palau,¹ Carlos E. Vera, and Julian I. Schroeder²

Division of Biological Sciences, Cell and Developmental Biology Section, and Center for Molecular Genetics, University of California, La Jolla, California 92093-0116

Among the >200 members of the leucine-rich repeat receptor kinase family in *Arabidopsis thaliana*, only a few have been functionally characterized. Here, we report a critical function in anther development for the *SOMATIC EMBRYOGENESIS RECEPTOR KINASE1* (*SERK1*) and *SERK2* genes. Both *SERK1* and *SERK2* are expressed widely in locules until stage 6 anthers and are more concentrated in the tapetal cell layer later. Whereas *serk1* and *serk2* single insertion mutants did not show developmental phenotypes, *serk1 serk2* double mutants were not able to produce seeds because of a lack of pollen development in mutant anthers. In young buds, double mutant anthers developed normally, but *serk1 serk2* microsporangia produced more sporogenous cells that were unable to develop beyond meiosis. Furthermore, *serk1 serk2* double mutants developed only three cell layers surrounding the sporogenous cell mass, whereas wild-type anthers developed four cell layers. Further confocal microscopic and molecular analyses showed that *serk1 serk2* double mutant anthers lack development of the tapetal cell layer, which accounts for the microspore abortion and male sterility. Taken together, these findings demonstrate that the *SERK1* and *SERK2* receptor kinases function redundantly as an important control point for sporophytic development controlling male gametophyte production.

INTRODUCTION

Plant life alternates between the sporophytic phase and the gametophytic phase represented by the female embryo sac and the male pollen grain. In flowers, special organs are dedicated to the transition from the sporophytic to the gametophytic phase and the maturation of female and male gametophytes. Anthers in *Arabidopsis thaliana* have a four-lobed structure, each containing a sporangium in which, early in development, two cell lines differentiate: (1) the germ line is a mass of cells that through sporogenesis and gametogenesis produces the male gametophytes and (2) the surrounding sporophytic tissues differentiate into four cell layers named from outside to inside, the epidermis, the endothecium, the middle cell layer, and the tapetum (Sanders et al., 1999; Ma, 2005). Several studies have shown that the surrounding four cell layers are crucial for the development of microsporocytes into mature pollen (Mariani et al., 1990; Burgess et al., 2002). Thus, mature anthers are highly organized

structures. However, the early steps in development that determine cell fate remain largely unknown (Ma, 2005).

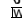
Plant organ development requires communication between cell layers to coordinate tissue differentiation (Fletcher, 2002; Larkin et al., 2003; Shpak et al., 2004, 2005; Chevalier et al., 2005). Receptor-like kinases (RLKs) (Shiu and Bleecker, 2001; Fritz-Laylin et al., 2005) are good candidates to coordinate these processes during anther development. Indeed, recent genetic studies showed that the plasma membrane-localized leucine-rich repeat receptor kinase (LRR-K) of the BRASSINOSTEROID-INSENSITIVE1 (BRI1) subfamily, EXCESS MICROSPOROCTES1/EXTRA SPOROGENOUS CELLS (EMS1/EXS), functions in the control of cell fate during anther development (Canales et al., 2002; Zhao et al., 2002). EMS1/EXS1 and BRI1 belong to subfamily X of the LRR-Ks (Shiu and Bleecker, 2001). Mutations in the *EMS1/EXS* gene cause an increased differentiation of anther cells in microsporocytes, affect anther wall organization, and lack the tapetal cell layer. Moreover, the same developmental phenotypes were observed for mutations in the *TAPETUM DETERMINANT1* (*TPD1*) gene, which encodes a predicted small secreted protein (Yang et al., 2003). *TPD1* could regulate cell fate in coordination with EMS1/EXS (Yang et al., 2005).

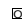
The *SOMATIC EMBRYOGENESIS RECEPTOR KINASE* (*SERK*) genes encode LRR-Ks belonging to the 14-member subfamily II of the LRR-Ks (Shiu and Bleecker, 2001). They share the canonical structure of LRR-Ks but have a limited number of LRR motifs. *Arabidopsis* *SERK3*, also named BAK1 (for BRI1-Associated Kinase1), was characterized as a component of brassinosteroid perception/signaling (Li et al., 2002; Nam and Li, 2002). Initial studies have shown that overexpression of *SERK1*

¹ Current address: Department of Plant Biology, Faculty of Pharmacy, Universitat de València, Burjassot-Valencia, Spain.

² To whom correspondence should be addressed. E-mail julian@biomail.ucsd.edu; fax 858-534-7108.

The author responsible for distribution of materials integral to the findings presented in this article in accordance with the policy described in the Instructions for Authors (www.plantcell.org) is: Julian I. Schroeder (julian@biomail.ucsd.edu).

 Online version contains Web-only data.

 Open Access articles can be viewed online without a subscription. Article, publication date, and citation information can be found at www.plantcell.org/cgi/doi/10.1105/tpc.105.036731.

enhances the ability of suspension cells to undergo somatic embryogenesis (Schmidt et al., 1997; Hecht et al., 2001). To date, nothing is known about the functions of the remaining members of the *Arabidopsis* LRR II subfamily.

In this study, we investigated the function of a functionally uncharacterized member of the LRR II family, *SERK2*, which is the closest homolog to *SERK1* and related to *SERK3/BAK1*. Phenotypic analyses of *serk1 serk2* double mutants show that *SERK1* and *SERK2* have a crucial and redundant function in anther development and male gametophyte maturation.

RESULTS

Identification of Single and Double Mutants in the *SERK1* and *SERK2* Genes

Overexpression of *SERK1* in *Arabidopsis* has been shown to enhance the efficiency of initiation of somatic embryogenesis of embryogenic cultures (Hecht et al., 2001). To identify loss-of-function-associated phenotypes in *SERK1* and *SERK2* genes, we obtained two *SERK1* and one *SERK2* insertional T-DNA mutant alleles from the Signal Collection at the Salk Institute (La Jolla, CA). They were named *serk1-1*, *serk1-2*, and *serk2-1* (Figure 1A). Sequencing of T-DNA insertion flanking borders showed that *serk1-1* has a tandem T-DNA insertion located in the

11th exon and an inframe stop codon 151 bp into the T-DNA insertion, and *serk1-2* has an insertion in the 11th exon and an inframe stop codon 55 bp into the T-DNA insertion. The predicted proteins *SERK1-1* and *SERK1-2* lack 103 and 74 C-terminal amino acids, respectively, corresponding to deletions in the kinase domain of 55 and 26 amino acids, respectively. In *serk2-1*, a tandem T-DNA insertion is located in the third intron (Figure 1A).

In order to assess the expression level of *SERK1* and *SERK2* in homozygous T-DNA lines, RT-PCR experiments were performed on bud cDNAs from the wild type and the homozygous double mutants *serk1-1 serk2-1* and *serk1-2 serk2-1* (Figure 1B). With *SERK1*-specific primers upstream of the T-DNA insertions, a PCR product was amplified for the double mutants as for the wild type. However, with primers surrounding the insertions, we were not able to amplify any product from *serk1-1* and *serk1-2* alleles (Figure 1B). Thus, in the double mutants, truncated transcripts were detected at low levels, but mature *SERK1* transcripts were undetectable. With *SERK2*-specific primers, two PCR products were amplified with primers designed either upstream or downstream of the insertion. With primers surrounding the insertion, two *serk2-1* products were amplified that showed low levels of expression compared with the wild type (Figure 1B). Sequencing of those products showed that the larger one was a wild-type transcript, whereas the shorter one was due to aberrant splicing

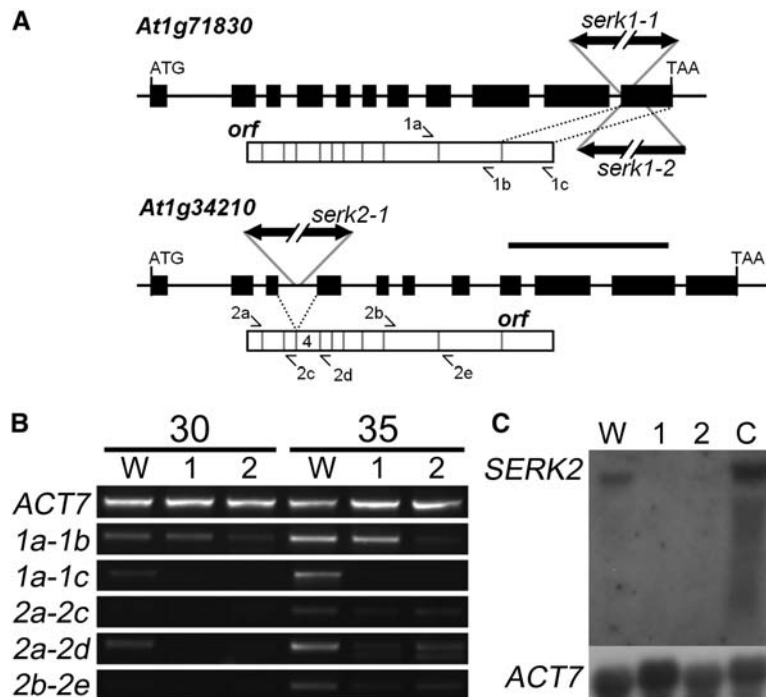


Figure 1. Characterization of *SERK1* and *SERK2* Loci.

(A) Genomic organization of *SERK1* and *SERK2* loci, predicted open reading frames (ORFs), and positions of primers used in Figure 1B. Left borders of T-DNAs are indicated by bold arrows. Bar = 1 kb.

(B) Expression of *SERK1* and *SERK2* in *serk1-1 serk2-1* and *serk1-2 serk2-1* plants using semiquantitative RT-PCR. The number of PCR cycles (30 to 35) is indicated on the top for the wild type (W) and the double mutants *serk1-1 serk2-1* (1) and *serk1-2 serk2-1* (2). Primer pairs are indicated at the left.

(C) RNA gel blot analysis of *SERK2* in the wild type (W), *serk1-1 serk2-1* (1), *serk1-2 serk2-1* (2), and a complemented line (C). Approximately 15 μ g of total mRNA from buds were loaded. Probes were full-length *SERK2* ORF (*SERK2*) and for controls, *ACTIN7* (*ACT7*).

causing the loss of exon 4 (Figures 1A and 1B). To better quantify the expression level of *SERK2* transcript in both *serk1-1 serk2-1* and *serk1-2 serk2-1*, we performed RNA gel blot experiments on bud mRNA. We were not able to detect expression of full-length or truncated *SERK2* transcript in double mutants, whereas full-length *SERK2* mRNA was detected in the wild type (Figure 1C). Thus, *serk2-1* mutation strongly reduces the *SERK2* transcript level and causes aberrant splicing, but the *serk2-1* mutant is likely not a null allele. Despite further efforts, we were unable to identify null alleles in publicly unrestricted accessible populations of insertional lines.

Despite multiple analyses, we were not able to unveil a dramatic phenotype for the *serk1* and *serk2* single mutants at the whole plant developmental level. This suggested that either the single mutants have subtle phenotypes or that *SERK* genes are functionally redundant to some extent. Indeed, *SERK1* and *SERK2* are closely related genes from the LRR-K encoding gene family and share 78.9 and 89.3% identity at the nucleotide and amino acid levels, respectively. We therefore analyzed the two double mutants *serk1-1 serk2-1* and *serk1-2 serk2-1*.

T-DNA Insertions in *SERK* Loci Trigger Sterility

During vegetative growth, *serk1-1 serk2-1* and *serk1-2 serk2-1* were indistinguishable from wild-type plants, and flowering times were not affected (data not shown). However, during the reproductive phase, both double mutants exhibited short fruits (Figure 2A) and did not produce any seeds.

In order to evaluate the genetic linkage of the two insertion loci to the observed sterility, we examined the progeny of the two different genotypes (*serk1-1 serk2-1* and *serk1-2 serk2-1*), which were either heterozygous for the *serk1* alleles or heterozygous for the *serk2-1* allele (Table 1). These parental genotypes were fertile

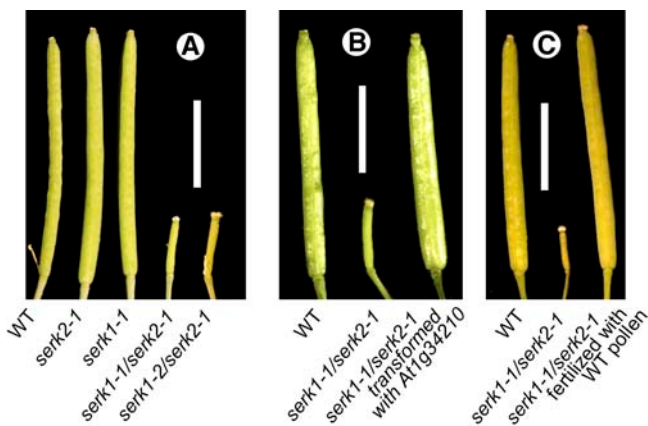


Figure 2. Siliques of *serk1 serk2* Double Mutants Do Not Produce Seeds.

(A) Developmental phenotype of siliques of single and double *serk1* and *serk2* mutants.

(B) Complementation of *serk1-1 serk2-1* siliques phenotype by *SERK2* genomic construct (At1g34210).

(C) *serk1-1 serk2-1* fertilization with wild-type pollen.

Bars = 5 mm.

($n > 30$ for each). Among the progeny, 16.7 to 27.9% of the plants were sterile (Table 1). All plants were PCR genotyped, and all of the sterile plants were homozygous for insertions at both the *SERK1* and *SERK2* loci (Table 1). All fertile plants carried at least one wild-type allele at the *SERK1* or *SERK2* locus with a ratio of $\sim 1:2$ (wild type:heterozygote), as expected for the segregation of a unique locus within the fertile and nonhomozygous plants ($\chi^2 < 1.89$). These results indicate that the phenotype is genetically linked to both the *SERK1* and *SERK2* loci and that the two mutations that trigger sterility are recessive. We identified two independent *serk1* mutant alleles that showed a similar sterile phenotype when combined with the *serk2-1* mutation. This result suggests that the disruption of *SERK1* was responsible for the sterile phenotype observed for double mutants. As *serk1* single mutants produced seeds and the sterile phenotype was observed only when *serk1* lines were crossed with the *serk2-1* line, *serk1* mutations need to be combined with a mutation that is genetically linked to *SERK2* to trigger sterility.

To determine whether mutation of the *SERK2* gene, when combined with *serk1* mutations, causes the sterile phenotype, we analyzed complementation of the *serk1 serk2* sterile phenotype. No complementation was obtained when the *SERK2* ORF was expressed under the control of the ectopic cauliflower mosaic virus 35S promoter, indicating that the noncoding sequences of the *SERK2* locus may contribute to *SERK2* function. Therefore, complementation with a genomic clone of the *SERK2* locus was pursued. We introduced a PCR-amplified genomic fragment containing the *SERK2* locus, which included 1442 bp upstream of the start codon and 1000 bp downstream from the stop codon in *serk1-1/SERK1 serk2-1/serk2-1* plants. Based on EST and cDNA database analyses, this genomic fragment contained no further ORFs apart from *SERK2*. We genotyped the transformed progeny to identify plants homozygous for *serk1-1* and *serk2-1* and found that they were able to produce seeds (Figure 2B). Complemented plants expressed full-length *SERK2* transcript (Figure 1C). Taken together, these findings demonstrate that the combination of *serk1* and *serk2* receptor kinase mutations triggers the sterile phenotype observed in the *serk1 serk2* double mutants.

serk1 serk2 Double Mutants Do Not Produce Pollen

To explore the cause of the *serk1 serk2* sterility, *serk1-1 serk2-1* double mutant pistils were fertilized with wild-type pollen. The sterile phenotype was rescued, allowing fruit development and the production of seeds (Figure 2C), and the resulting seedlings were all heterozygous for both insertion loci ($n = 16$; data not shown). These findings, together with the above genetic analyses, show that the *serk1 serk2* mutations trigger male sterility.

We further investigated anther development. Double mutant *serk1 serk2* nondehiscent open flowers had six anthers that were smaller than wild-type anthers (data not shown). Alexander's solution, which stains pollen cytosol red to monitor pollen viability (Alexander, 1969), was applied to open flowers. Viable pollen grains clearly appeared in the wild type, in *serk1* and *serk2* single mutants, and in the complemented *serk1-1 serk2-1* double mutant lines (Figure 3A). However, we did not detect any staining in *serk1 serk2* double mutant anthers, indicating that *serk1 serk2*

Table 1. Sterility Phenotype and Mutant Genotypes Are Linked

Parental Genotype	Progeny Phenotype ^a	Progeny Genotype ^b					
		SERK1 (%)			SERK2 (%)		
		+/+	+/-	-/-	+/+	+/-	-/-
<i>S1/s1-2 s2-1/s2-1</i>	50 (83.3) fertile	42.0	58.0	0	0.0	0.0	100
	10 (16.7) sterile	0.0	0.0	100	0.0	0.0	100
<i>S1/s1-1 s2-1/s2-1</i>	31 (72.1) fertile	38.7	61.3	0	0.0	0.0	100
	12 (27.9) sterile	0.0	0.0	100	0.0	0.0	100
<i>s1-1/s1-1 S2/s2-1</i>	32 (78) fertile	0.0	0.0	100	21.9	78.1	0
	9 (22) sterile	0.0	0.0	100	0.0	0.0	100
<i>s1-2/s1-2 S2/s2-1</i>	41 (77.4) fertile	0.0	0.0	100	26.8	73.8	0
	12 (22.6) sterile	0.0	0.0	100	0.0	0.0	100

Genetic analyses of the segregating progeny of *serk1 serk2* double mutants with one heterozygous insertion. *S1*, *SERK1*; *S2*, *SERK2*; *s1-1*, *serk1-1*; *s1-2*, *serk1-2*; *s2-1*, *serk2-1*; +, wild-type allele; -, mutant allele. The percentages of individual phenotypes (sterile/fertile) are given in parentheses.

^a The progeny phenotypes (fertile:sterile) in all cases fit a 3:1 hypothesis with 5% confidence ($\chi^2 < 2.22$).

^b When applicable, the progeny genotype values (wild type:heterozygote) fit a 1:2 hypothesis with 5% confidence ($\chi^2 < 1.89$).

anthers did not produce pollen (Figure 3A). Moreover, sections in mature anthers reveal the collapsing of the four microsporangia in *serk1-1 serk2-1* double mutants (Figure 3B). To examine possible differences in the development of wild-type and mutant pollen, young floral buds were cleared using a protocol that allows examination and optical sectioning of whole anthers (see Methods). In wild-type flowers, premeiotic, tetrad, and mature pollen stages were all identifiable (stages 6, 7, 9, and 10, respectively; Figures 3C, 3E, and 3G). In *serk1-1 serk2-1* double mutant anthers at the same stage (based on the size of microsporangia), we observed the same premeiotic structure (Figure 3D). But, unlike wild-type plants, these premeiotic structures appeared to be arrested during development. *serk1-1 serk2-1* double mutant anthers did not show the formation of the characteristic imbricated microspores organized as clear multiple distinguishable tetrads at stages 7 (Figure 3F), 10 (Figure 3H), or later (data not shown). However, at this stage, it remains unclear whether initial tetrad-like structures may form or not and whether meiosis does occur or not in double mutant anthers (see below). In addition, some alterations of the anther wall were observed in *serk1 serk2* and are described later.

***serk1 serk2* Double Mutants Produce an Increased Number of Microsporocytes That Undergo Meiosis**

We investigated the number of sporogenous cells in young locules (stages 4 to 6) by optical sectioning of propidium iodide-stained anthers. We found that the wild type had 17.7 ± 1.3 (\pm SE, $n = 26$) microsporocytes per microsporangium. By contrast, *serk1-1 serk2-1* and *serk1-2 serk2-1* showed a significantly increased number of microsporocytes: 26.0 ± 2.9 ($n = 23$) and 26.6 ± 2.2 ($n = 22$), respectively. Both wild-type and double mutants were characterized by a large variability in microsporocyte numbers among microsporangia. Nevertheless, whereas we did not find any microsporangia with ≥ 31 microsporocytes in wild-type stamens, 43.5% in *serk1-1 serk2-1* and 40.9% in *serk1-2 serk2-1* showed between 30 and 50 nuclei (Figure 4A).

Optical sectioning of propidium iodide-stained anthers showed that both wild-type and double mutant microsporocytes were able to undergo meiosis. Cells with one, two, and four nuclei were observed in both wild-type and *serk1-1 serk2-1* mutants corresponding to the product of the first and second meiotic divisions (Figure 4B). At later stages, the wild type showed microspores organized in well-defined tetrad structures (Figure 4C, top), which then developed into pollen grains (Figure 4C, bottom). Comparable well-developed multiple tetrad structures were not observed in *serk1 serk2* at this stage, but instead separated cells were observed (Figure 4D, top) that degenerated after meiosis (Figure 4D, bottom). These data indicate that *SERK1* and *SERK2* function in the control of male germ line cell numbers during anther morphogenesis but perhaps not directly in male germ line fate.

Tapetum Development Is Impaired in *serk1 serk2*

High-resolution confocal microscopy revealed another impairment of *serk1 serk2* double mutant anthers. Whereas in young anthers (stage 5) four cell layers surrounded the sporogenous cell mass in wild-type stamens (Figure 5A), interestingly only three cell layers surrounding *serk1-1 serk2-1* double mutant microsporangia could be identified (Figure 5B).

The four cell layers were morphologically distinguishable during development of wild-type anthers. Interestingly, confocal observation of more mature wild-type microsporangia (stage 6) (Sanders et al., 1999) showed that cell layer 3 is flattened with the development of the neighboring cell layers and its nuclei appear flat as well (Figures 5A and 5D). The flat cells remain until stage 10 (Figure 5F). The tapetum develops as a thick and autofluorescent cell layer (Figures 5C to 5F) and undergoes a last nuclear division leading to cells with two separated nuclei (Figures 5C to 5E) (Yang et al., 1999; Weiss and Maluszynska, 2001).

In early stages of *serk1 serk2* double mutant anther development, we did not observe the flattened middle cell layer surrounding the pretapetal cells found in the wild-type anthers

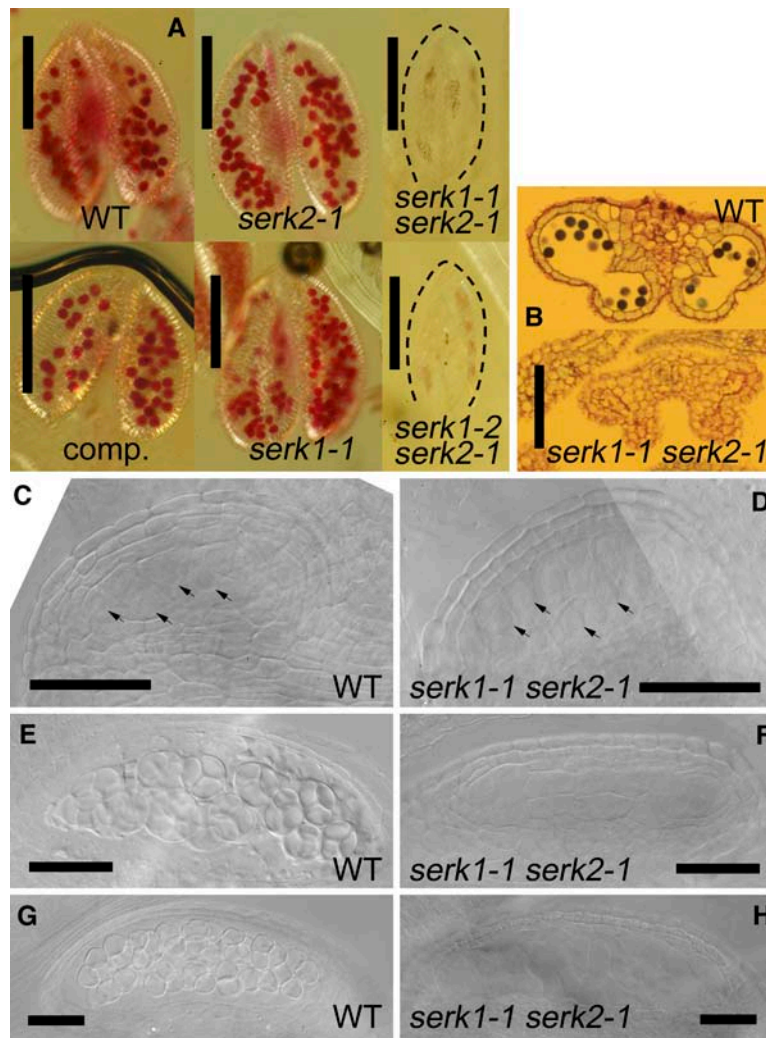


Figure 3. *serk1 serk2* Double Mutants Do Not Produce Pollen.

(A) Transmission microscopy observation of dehiscence-stained stamens of wild-type, *serk1-1*, and *serk2-1* single mutants, *serk1 serk2* double mutants, and a *SERK2* complemented line (comp.). Flowers were stained with Alexander's solution (1 h) and cleared using Herr's buffer (1 h). Dashed lines surround the double mutant anthers for clarity.

(B) Toluidine blue staining of 8- μ m-wide sections in mature stamens of the wild type and *serk1-1 serk2-1* shows the collapse of microsporangia in *serk1-1 serk2-1*.

(C) to (H) Differential interference contrast observations of Herr-cleared whole stamens show an early termination of development in the *serk1-1 serk2-1* double mutants ([D], [F], and [H]) compared with the wild type ([C], [E], and [G]). Photographs were taken at premeiotic (stage 5) ([C] and [D]), tetrad (stage 7) ([E] and [F]), and post-tetrad stages (stage 11) ([G] and [H]). Developmental stages of *serk1-1 serk2-1* were identified based on microsporangium size. In (C) and (H), arrows point to microsporocyte nuclei.

Bars = 200 μ m in (A) and (C) to (H) and 100 μ m in (B).

(3 and 4 in Figure 5A), but instead, we observed a single cell layer with globular nuclei (3 in Figure 5B). At later stages, this cell layer persists (Figure 5G). Moreover, whereas in wild-type anthers an accumulation of autofluorescent material was visible between the middle cell layer and the tapetum (Figures 5D and 5E, arrowheads), in the *serk1 serk2* mutants, accumulation of autofluorescence was facing the inside of the microsporangia (Figure 5G, arrowheads). These observations led us to hypothesize that the tapetal cell layer is missing in anthers of the *serk1-1 serk2-1*

mutant. Moreover, the third cell layer of the double mutant (3 in Figure 5B) does not morphologically develop as the middle cell layer.

Expression of Tapetum-Specific Genes Is Strongly Impaired in *serk1 serk2* Double Mutants

To test the hypothesis that the tapetum is absent in *serk1 serk2* double mutants, we investigated a set of genes reported to be

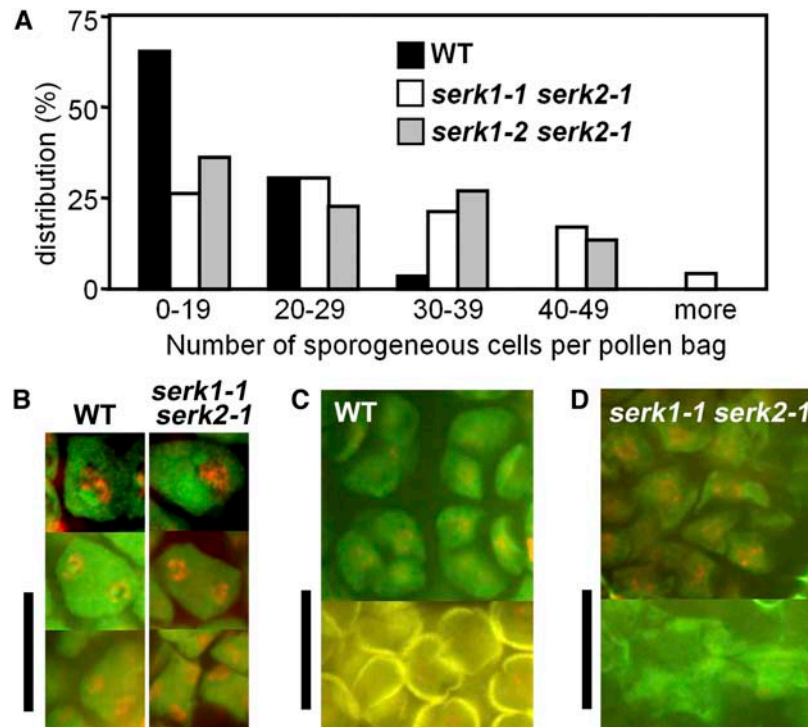


Figure 4. *serk1 serk2* Microsporangia Contain More Microsporocytes Than the Wild Type.

(A) Population distribution of the number of sporogenous cells per microsporangium in wild-type and *serk1 serk2* double mutants. Note the large number of sporogenous cell mass with ≥ 30 microsporocytes in *serk1 serk2* double mutant anthers compared with the wild type.

(B) Propidium iodide staining of the locule content of wild-type and *serk1-1 serk2-1* whole anthers. Both wild-type (left panels) and *serk1-1 serk2-1* (right panels) microsporocytes undergo meiosis. From top to bottom panels: meiotic cells with one, two, and four nuclei (three are in the same confocal section).

(C) and **(D)** Whereas the wild type showed microspores organized in well-defined multiple tetrad structures (**[C]**, top panel), which differentiated later into pollen grains (**[C]**, bottom panel), *serk1-1 serk2-1* showed less-organized microspores (**[D]**, top panel), which degenerated (**[D]**, bottom panel). Propidium iodide-stained nuclei are shown in red and tissue autofluorescence in green.

Bars = 40 μm in **(B)** to **(D)**.

specifically transcribed in the tapetal cell layer in inflorescences of wild-type and both double mutant plants by semiquantitative RT-PCR. The following tapetum-specific mRNA levels were analyzed: *ARABIDOPSIS THALIANA ANTHER7* (*ATA7*; Rubinelli et al., 1998), *MALE STERILITY1* (*MS1*; Wilson et al., 2001; Ito and Shinozaki, 2002), *LYSINE HISTIDINE TRANSPORTER1* (*LHT1*; Chen and Bush, 1997), and *QUARTET3* (*QRT3*; Rhee et al., 2003). As a control, we made use of *ACTIN7*, which is expressed throughout plant tissues. Whereas *ACTIN7* showed similar expression in wild-type and both *serk1 serk2* mutants (Figure 6A), the expression levels of *ATA7*, *MS1*, *QRT3*, and, to a lesser extent, *LHT1* were either virtually absent or reduced in the double mutant inflorescences (Figures 6A and 6B). These expression data are in agreement with the confocal microscopy analyses (Figures 4 and 5) and further support the notion that the tapetum is absent from anthers in *serk1 serk2* double mutants.

SERK1 and SERK2 Are Expressed in Anther Locules

RT-PCR and microarray analyses showed that *SERK1* and *SERK2* are expressed in all aerial organs and particularly

in flowers and siliques (Figure 7A). *serk1 serk2* double mutants showed a tissue-restricted phenotype, indicating that *SERK1* and *SERK2* transcripts may be abundant in specific cells within the anther. We generated transgenic lines expressing the β -glucuronidase gene (*GUS*) under the control of a 1.5-kb fragment of the *SERK2* promoter. Only few lines (4 of 70) exhibited a weak blue staining, suggesting, together with the difficulty of *SERK1* and *SERK2* mRNA detection by RNA gel blots, that *SERK1* and *SERK2* are low abundance transcripts. Cross sections of *SERK2 promoter-GUS* lines showed that the *SERK2* promoter triggers broad gene expression in stage 6 anthers (Figure 7B) but is restricted to the tapetal cell layer at later stages (stage 9; Figure 7C).

The low expression level of *SERK2* was also confirmed by analyzing data from digital Northern, which have integrated 1401 (in February, 2005) Affymetrix microarray experiments (Zimmermann et al., 2004). These 1401 microarray experiments were analyzed for correlations of *SERK1* or *SERK2* expression levels with expression levels of the tapetum-specific *ATA7* gene. These analyses showed a degree of correlation of *SERK1* and *SERK2* expression to high *ATA7* expression values and further

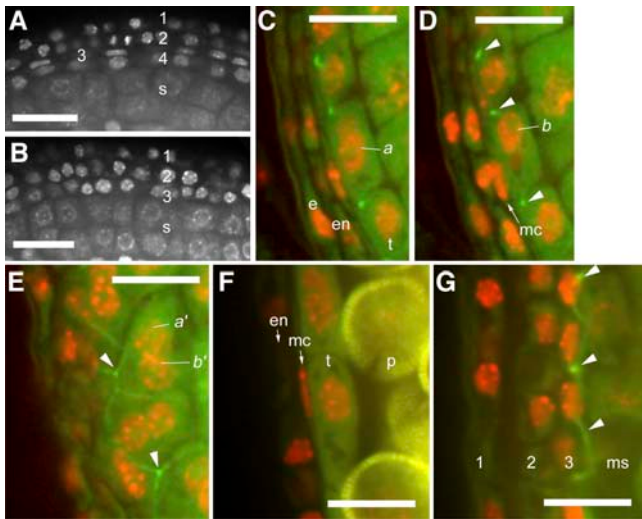


Figure 5. Absence of Tapetal Cell Layer in *serk1 serk2* Double Mutants.

(A) Propidium iodide–stained wild-type microsporangium (stage 5) showing the four cell layers of the anther wall. 1, 2, 3, and 4 refer to the cell layers: 1, epidermis; 2, endothecium; 3, middle cell layer; 4, tapetum.

(B) Propidium iodide–stained *serk1-1 serk2-1* microsporangium at stage 5 exhibits only three cell layers of the anther wall. 1, 2, and 3 refer to surrounding cell layers.

(C) to (F) Optical sections of propidium iodide–stained microsporangia of the wild type at stages 5 and 6 [(C) to (E)] and stage 10 (F). Red is propidium iodide staining (600 nm), and green is autofluorescence (510 nm). (C) and (D) show 1- μ m-separated optical sections perpendicular to a wild-type microsporangium. (E) shows an optical section tangential to the tapetum cell layer from the same Z-stack as (C) and (D). a, b, a', and b' are examples of two nuclei in the same cells. Arrowheads show the characteristic autofluorescence of cell wall surrounding tapetum cells. (F) is an optical section in a stage 10 wild-type locule showing persistence of the middle cell layer at an advanced stage of development. Note that the epidermal cell layer often detaches from mature stamens.

(G) Optical sections of propidium iodide–stained microsporangium of *serk1-1 serk2-1* at stages 8 to 10. Numbers indicate the three cell layers. Arrowheads point to autofluorescence of the double mutant anther wall. s, sporogenous cells; e, epidermis; en, endothecium; t, tapetum; mc, middle cell layer; p, pollen; ms, microspores. Bars = 20 μ m in (A) and (B) and 10 μ m in (C) to (G).

indicate that *SERK* genes are expressed more widely than the tapetum-specific gene *ATA7* (see Supplemental Text 1 and Supplemental Figure 1 online; Rubinelli et al., 1998; Shiu and Bleecker, 2001; Canales et al., 2002; Zhao et al., 2002; Zimmermann et al., 2004) in agreement with RT-PCR experiments (Figure 7A). Furthermore, expression analyses of the same 1401 experiments show that elevated expression levels of *SERK1* and *SERK2* correlate with high expression levels of the EMS1/EXS receptor kinase gene in a subset of experiments (see Supplemental Figure 1 online).

We further investigated *SERK1* and *SERK2* tissue expression using RNA in situ hybridizations. *SERK1* RNA (Figure 7D) but not *SERK2* (Figure 7E) was detected in stamen primordia (stage 2). In

older buds, both transcripts are present in locules of stage 4 to 5 anthers, including expression in sporogenous cells and tapetum and also more external cell layers, including the endothecium and middle cell layer (Figures 7F and 7G). At stage 5 to 6, both transcripts were more concentrated in the tapetal cell layer and apparently also the middle cell layer (Figures 7H and 7I). Then, the hybridization signals faded once meiosis occurred (stages 8 to 9; data not shown). As a positive control, the expression of a gynoecium-specific gene was analyzed in parallel by in situ hybridizations (B. Crawford and M.F. Yanofsky, unpublished data). As expected, the gynoecium-specific transcript was not detected in anther locules (data not shown) and therefore differed from the expression pattern of *SERK1* and *SERK2* transcripts (Figures 7F to 7I). In addition, like *SERK1* (Shah et al., 2001), *SERK2* is expressed in ovules (data not shown).

This pattern of *SERK1* and *SERK2* expression is in accordance with *SERK*-yellow fluorescent protein fusion data presented in Albrecht et al. (2005) and Kwaaitaal et al. (2005). The authors show a wide expression of *SERK* genes in locules at early stages that faded by the end of stage 5 in the microsporocytes. Small differences, such as expression at late stages that included the epidermal cell layer and endothecium observed using protein-YFP fusions but not in in situ hybridizations, may reflect either

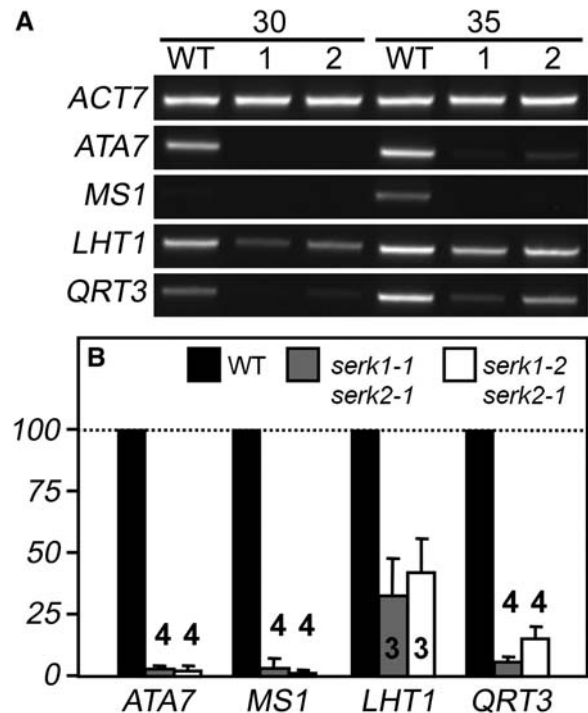


Figure 6. Expression of Tapetum-Specific Genes Is Strongly Reduced in *serk1 serk2*.

(A) Semiquantitative RT-PCR analyses of *ACT7*, *ATA7*, *MS1*, *LHT1*, and *QRT3* expression in the wild type, *serk1-1 serk2-1* (1), and *serk1-2 serk2-1* (2). The number of PCR cycles (30 and 35) is indicated at the top.

(B) Quantification and normalization of RT-PCR signals to wild-type levels for the indicated genes. Histograms are mean \pm SE. Numbers of experiments are indicated for each condition.

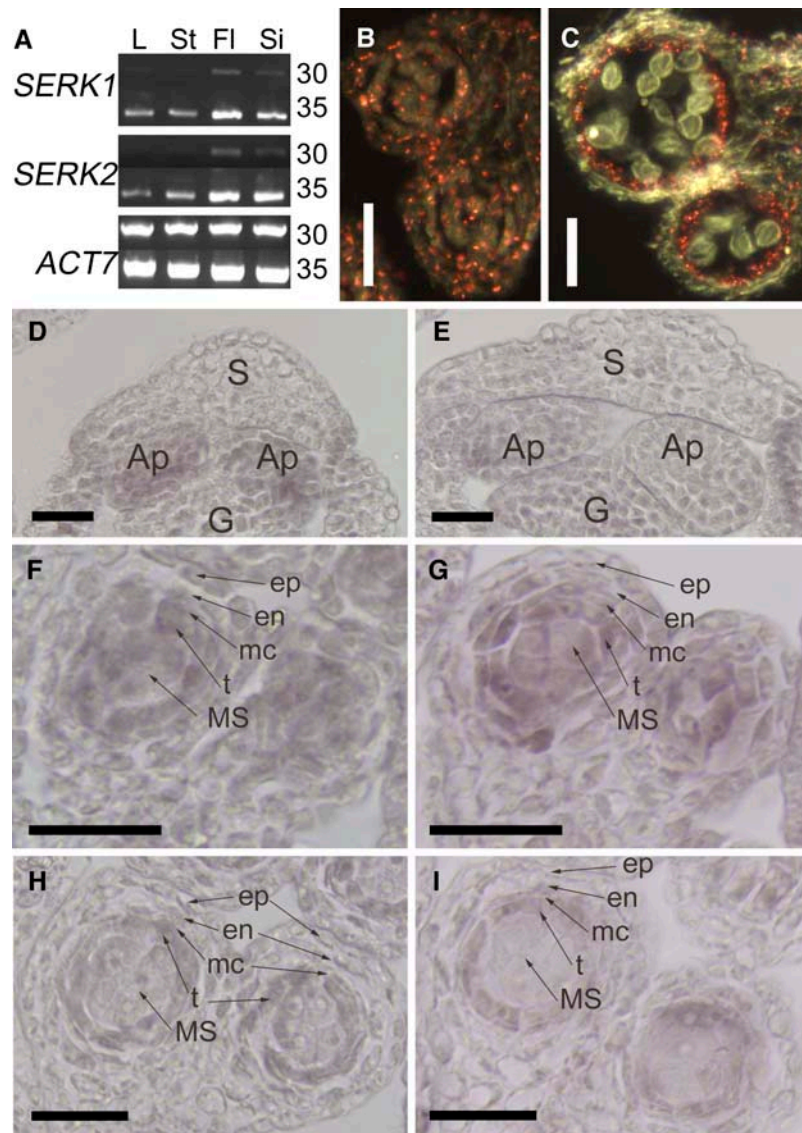


Figure 7. *SERK1* and *SERK2* Expression in Anthers.

(A) Semiquantitative RT-PCR analyses of *ACT7*, *SERK1*, and *SERK2*. The number of PCR cycles (30 and 35) is indicated at right. The primer pair used for *SERK1* was 1a and 1b, as illustrated in Figure 1A, and for *SERK2*, the primer pair was 2b and 2e from Figure 1A (Table 2). L, leaves; St, stem; Fl, flowers; Si, siliques.

(B) and **(C)** Expression of GUS under the control of *SERK2* promoter in stage 6 **(B)** and stage 9 **(C)** stamens.

(D) to **(I)** Expression of *SERK1* **(D)**, **(F)**, and **(H)** and *SERK2* **(E)**, **(G)**, and **(I)** in anthers examined by in situ hybridization in transversal sections. *SERK1*, but not *SERK2*, is expressed in locules of stage 2 anthers **(D)** and **(E)**. *SERK1* and *SERK2* are expressed widely in locules of stage 4 to 5 anthers **(F)** and **(G)** and in the tapetum of stage 5 to 6 anthers **(H)** and **(I)**. S, sepal; Ap, anther primordium; G, gynoecium; ep, epidermis; en, endothecium; t, tapetum; mc, middle cell layer; MS, microsporocyte.

Bars = 250 μ m in **(B)** to **(I)**.

technical limitations of both approaches or a divergence between the abundances of *SERK* transcripts and *SERK* proteins. Nevertheless, both studies gave a similar general expression pattern for *SERK1* and *SERK2* in anthers; namely, at first, a wide expression in the locules at early stages, including microsporocytes, and later an expression restricted to surrounding cell layers.

DISCUSSION

In this study, we report the characterization of redundant *SERK1* and *SERK2* functions during organ development. The combination of *serk1* and *serk2* mutations triggers male sterility characterized by a lack of pollen production, showing functional redundancy among these two LRR-K encoding *SERK* genes.

Confocal analyses of propidium iodide-stained microsporangia showed that *serk1 serk2* double mutant microsporangia contained more microsporocytes than the wild type. However, *serk1 serk2* double mutants contained only three cell layers surrounding the microsporangia instead of the characteristic four cell layers. High-resolution microscopic and molecular investigations showed that the missing cell layer is the tapetum. The lack in tapetum development can explain the degeneration at later stages of the sporogenous cells and the ensuing male sterility.

serk1 serk2* Show Phenotypes Related to *tpd1* and *ems1/exs

serk1 serk2 double mutants exhibit a lack of development of the tapetal cell layer. The lack of the tapetal cell layer is similar to other mutants described as male sterile, which do not produce any pollen because of either a tapetum function failure or its absence. Previous tapetum ablation studies demonstrated that the presence of the tapetum is essential for pollen production (Koltunow et al., 1990; Mariani et al., 1990). The *sporocyteless/nozzle* (*spl/nzz*) mutants are mutated in a nuclear factor necessary for male and female sporangium development (Schieffhale et al., 1999; Yang et al., 1999). In *spl/nzz*, at a very early stage, the anther wall fails to develop and microspores do not differentiate. *MS1* encodes a tapetum-expressed plant homeodomain-finger transcription factor (Wilson et al., 2001; Ito and Shinozaki, 2002), and *NO EXINE FORMATION1* encodes an unknown protein likely involved in lipid metabolism (Ariizumi et al., 2004). These two genes seem to function in pollen feeding and maturation once differentiation of the tapetal cell layer has occurred.

In contrast with the above mutations, *ems1/exs* and *tpd1* are phenotypically similar to *serk1 serk2* double mutants: both fail to produce pollen because of the lack of tapetal cell layer development, and both produce more sporogenous cells that degenerate after meiosis (Canales et al., 2002; Zhao et al., 2002; Yang et al., 2003; Ma, 2005). In addition, *ems1/exs* exhibits smaller embryos in mature seeds, a phenotype not observed in *serk1 serk2* double mutants (data not shown) and not reported for *tpd1* (Yang et al., 2003).

The model describing early anther development in *Arabidopsis* proposes that an early cell division separates sporogenous cells from cells that differentiate into the three inner cell layers of the anther wall (Canales et al., 2002; Zhao et al., 2002; Yang et al., 2003, 2005; Ma, 2005). In *ems1/exs* and *tpd1* anthers, the precursors of tapetal cells develop into microsporocytes instead of the tapetum (Zhao et al., 2002; Yang et al., 2003). This suggests that EMS1/EXS and TPD1 proteins function in the developmental fates of the tapetal precursors and likely not in the mitotic processes leading to the physical separation of cell layers. Our results on the *serk1 serk2* double mutant support this published model of position-dependent differentiation of tapetum cells and sporogenous cells (Ma, 2005). Nevertheless, an alternative explanation could be that the developing tapetum produces a signal to negatively regulate microsporocyte proliferation. In this later model, *serk1 serk2* mutants that lack the tapetal cell layer would have as a secondary phenotypic trait an altered number of microsporocytes triggered by a cell-to-cell communication failure. Time-dependent cell lineage studies using cell type-specific markers and confocal microscopy may help to further analyze these two hypotheses.

Confocal analyses of wild-type anthers in this study showed that the middle cell layer persisted throughout stage 10 as a flat cell layer surrounding the tapetum (Figure 5). Previous findings show middle cell layer degeneration at stages 6 and 7 (Sanders et al., 1999). Confocal microscopy may enhance resolution or growth, and other experimental conditions may slightly affect the stage of degeneration. The inner cell layer in *serk1 serk2* double mutants (3 in Figure 5B) never became flat, indicating either that the flattening may be a mechanical consequence of tapetum development or that the inner cell layer of the mutant is not comparable to cell layer 3 of wild-type anthers. Further analyses of the flattening of the middle cell layer identified here may lead to new insights into mechanisms during anther development and functions of SERK1 and SERK2.

Whereas several genes have been identified showing specific expression in the tapetal cell layer, no genes have been identified that are specifically expressed in the middle cell layer or the endothecium, two cell layers with still unknown functions.

Table 2. Primers Used for RT-PCR

Primer Name (AGI) ^a	Sequence (from 5' to 3')
1a (At1g71830)	GCCGAAGAAGATCCAGAAGTTCATC
1b (At1g71830)	TCCGCGTTGGCCAATCAAGCGGAGG
1c (At1g71830)	TTACCTTGGACCAGATAACTCAACGGCG
2a (At1g34210)	GTCTGCTTAATCTCACTGCTTCTTCTG
2b (At1g34210)	GCCGAAGAGGACCCCTGAGGTTCACT
2c (At1g34210)	AGTACTGCAAGTCTTGAGCTGACCTAG
2d (At1g34210)	GTCAATGACATGGGAATTGGTCC
2e (At1g34210)	TCTTATTGACCAAGGCTAGAGGCAAC
ATA7-F/ATA7-R (At4g28395)	TCACCTTCGCTAGCTAGTGTA/GTTACAAGGCTTCCCTTC
QRT3-F/QRT3-R (At4g20050)	GAGTCTAATGGTGAGTCAAGTGGTCTTC/GCACGCCGGACAATAAGTTAGCTTGTC
MS1-F/MS1-R (At5g22260)	GAGCCCATCGAAGCCTCTCAATCTC/GACTCTTTTCAGTGACTCTATGACCACT
LHT1-F/LHT1-R (At1g24400)	ATGGGGAACAGTGAATGTACAGCGAG/CACATTGGGACCTGGATGGCATCTC
ACTIN7-F/ACTIN7-R (At5g09810)	GGCCGATGGTGAGGATATTCAGCCACTTG/TCGATGGACCTGACTCATCGTACTCACTC

^aAGI, Arabidopsis Genome Initiative.

Identification of cell layer-specific expression markers would greatly help to characterize the *serk1 serk2* phenotypic class of mutants. Expression analyses of the tapetum-specific genes *ATA7*, *MS1*, *QRT3*, and *LHT1* provide molecular evidence that the missing cell layer in *serk1 serk2* is the tapetum (Figure 6; see Supplemental Figure 1 online).

SERK Genes and Functional Redundancy

We show a largely overlapping pattern of expression of *SERK1* and *SERK2* genes within the locules of developing anthers (Figure 7). In addition, using a *SERK2*-green fluorescent protein fusion, we detected a large fraction of *SERK2* protein in the plasma membrane and additional expression in endomembranes (data not shown). Nevertheless, expression analyses show that both *SERK* genes are expressed more widely in *Arabidopsis*, for example, in ovules (data not shown) and in leaves (Figure 7). Whereas *serk1 serk2* double mutants showed an anther-specific phenotype and did not clearly affect other aspects of growth or development analyzed in this study, the *SERK1* and *SERK2* genes are more broadly expressed (Figure 7A; see Supplemental Figure 1 online). The male sterile phenotype of *serk1 serk2* double mutants may also limit the resolution of further developmental phenotypes. Overexpression of *SERK1* has previously been shown to enable somatic embryogenesis in culture (Schmidt et al., 1997; Hecht et al., 2001). Both *SERK1* and *SERK2* transcripts are expressed in guard cells (Leonhardt et al., 2004), but double mutants showed no stomatal development or signal response phenotypes (data not shown). Thus, the *SERK* proteins may have other functions in planta, but either the corresponding phenotypes are weak or are masked by genetic redundancies with other LRR-Ks of the same subfamily II that has 14 members or by functional redundancies with other proteins and network pathways.

Do LRR-Ks of the Families II and X Function as Complexes?

The phenotypic similarities of *tpd1*, *ems1/exs*, and *serk1 serk2* mutants suggest that *SERK1* and *SERK2* could function in coordination with the *ems1/exs* and *TPD1* gene products during anther development. LRR-Ks are thought to interact with each other in a specific manner (Dievart et al., 2003; Shpak et al., 2003; Wang et al., 2005b). The involvement of two LRR-K classes in the same developmental process is intriguing, and interaction between those two LRR-K proteins could occur during anther formation to constitute a functional receptor. Independent findings support this hypothesis. Like *BAK1/SERK3*, *SERK2* and *SERK1* belong to the LRR II subfamily (Hecht et al., 2001). *BAK1/SERK3* was shown to interact with *BRI1*, an LRR-RLK belonging to the LRR X subfamily, to constitute a functional brassinosteroid receptor complex (Li et al., 2002; Nam and Li, 2002; Wang et al., 2005a) with the extracellular domain of *BRI1* functioning as a brassinolide binding protein (Kinoshita et al., 2005). Interestingly, like *BRI1*, the *EMS1/EXS* protein is a member of the LRR-K X subfamily. Consequently, it is tempting to suggest a model in which RLKs of the LRR-X (*BRI1/EMS1/EXS*) subfamily can interact with specific members of the LRR II (*SERK/BAK1*) subfamily, giving rise to functional perception systems in plants.

Albrecht et al. (2005) have independently identified *serk1 serk2* double mutants as lacking the tapetal cell layer and also show *SERK1* and *SERK2* functions during anther development.

METHODS

Plant Growth Conditions and Mutant Line Genotyping

Arabidopsis thaliana plants (ecotype Columbia 0) were grown in a Conviron growth chamber in plastic pots filled with ready-to-use soil (Professional Blend). After sowing, pots were kept at 4°C for 4 to 7 d. Growing conditions were 22°C and 75% humidity with a 16-h-light/8-h-dark photoperiod regime at $\sim 75 \mu\text{E}\cdot\text{m}^{-2}\cdot\text{s}^{-1}$.

serk2-1 (Salk_058020), *serk1-1* (Salk_044330), and *serk1-2* (Salk_053021) alleles of the At1g34210 and At1g71830 genes were obtained from the Signal Collection at the Salk Institute. Genotyping PCR reactions for single and double mutants were performed using 5'-GTCTGCTTAATCTCAC-TGCTTCTCTG-3'/5'-GTCAATGACATGGGAATTGGTCC-3' and 5'-GAG-CTACAAGTGGCGAGTGATGG-3'/5'-CGACGCTGTTTCGCTTTTGTG-3' primer pairs for *SERK2* and *SERK1*, respectively, which were mixed with *Lba1* (5'-TGGTTCACGTAGTGGGCCATCG-3') primers of the T-DNA to genotype plants in one reaction. Because both homozygous mutations in the double mutants led to a sterile phenotype, the segregating progenies of homozygous plants for one locus and heterozygous for the other locus were analyzed.

Plant Expression and Transformation

For the *SERK2* gene promoter reporter fusion, a 3.3-kb fragment of the *SERK2* locus was PCR amplified using 5'-CCAGATCCGAATCG-GACTCTTAAGTGTGCAC-3'/5'-CCATGGACCAAAAAAGCAAATTTCT-CCTCCCAG-3' primers, introducing a *NcoI* site (underlined) and cloned in pGEM-T easy (Promega). A 1.5-kb fragment was subcloned in pCAMBIA1303 (CAMBIA) using *EcoRI* and *NcoI* sites. For GUS activity assays, inflorescences were incubated in 80% acetone for 30 min at room temperature, washed three times with 50 mM phosphate buffer/0.1% Triton X-100, and incubated in the same buffer supplemented with $1 \text{ mg}\cdot\text{mL}^{-1}$ 5-bromo-4-chloro-3-indolyl- β -D-glucuronic acid overnight at 37°C. For cross sections, inflorescences were then fixed in FBA for 4 h then dehydrated with increasing ethanol solutions. Ethanol was progressively replaced by HistoClear II (National Diagnostics) and HistoClear II by Paraplast Embedding Media (Sigma-Aldrich). Eight-micrometer sections were stained with Toluidine blue (0.5% for 30 s) and mounted in Permount (Fisher Scientific).

For genomic complementation, a 6129-bp fragment was PCR amplified from the F23M19 BAC clone using the 5'-CTCGAGAATATTGG-TATGTGTTGTGTTTCACGTGAG-3'/5'-CTCGAGCCG TCTGAGAACCCT-TTCCATGCTCCCTC-3' pair of primers (the introduced *XhoI* site is underlined), cloned in pCR-Blunt (Invitrogen), and sequenced. This fragment was then subcloned using *XhoI* in pGREENII-0229 (Hellens et al., 2000). After confirmation by restriction digest, *Arabidopsis* transformation was performed by floral dipping with *Agrobacterium tumefaciens* carrying pSOUP and the *SERK2* genomic construct as previously described (Clough and Bent, 1998). Because *serk1-1 serk2-1* plants were unable to produce seeds, we transformed the progeny of a *serk1-1/SERK1 serk2-1/serk2-1* plant. Transformants were identified by Basta selection and genotyped by PCR as described above in order to identify the homozygous *serk1-1 serk2-1* plants.

Expression Analyses

Total RNAs were extracted using Trizol and quantified by absorption and migration of an aliquot on a gel. For RNA gel blots, total RNA was

separated in a denaturing formaldehyde-agarose gel and blotted to a Hybond N⁺ membrane (Amersham Pharmacia). Blots were hybridized with random-priming ³²P-labeled probes (Megaprime DNA labeling system; Amersham Pharmacia). Full-length *SERK2* ORF probe was amplified by PCR from a plasmid containing *SERK2* ORF using 5'-ATGGGG-AGAAAAAGTTTGAAGCTTTTGGTTTT-3'/5'-TTATCTTGGACCAGAC-AACTCCATAGC-3' primers. *ACTIN7* probe was amplified by PCR from cDNA using 5'-GGCCGATGGTGGGATATTCAGCCACTTG-3'/5'-TCG-ATGGACCTGACTCATCGTACTCACTC-3'. PCR fragments were purified using the QIAEX II kit (Qiagen).

For RT-PCR, 10 µg were treated with RNase-free DNase using the DNA-free kit (Ambion) and used to produce cDNA. Thirteen microliters of DNA-free RNA (0.77 µg·µL⁻¹) were incubated for 5 min at 70°C with oligo(dT) and chilled on ice before adding 0.5 µL RNase inhibitors (RNasin Plus; Promega), deoxynucleotide triphosphates to a final concentration of 0.5 mM each, M-MLV reverse transcriptase buffer, and 200 units of M-MLV reverse transcriptase (Promega) in a final volume of 25 µL. The cDNA mixes were incubated for 2 h at 37°C, diluted five times, and kept at -20°C prior to use. For each experiment, 5 µL of the cDNAs were used per reaction, and PCR premixes were carefully done to avoid bias between samples for a final volume of 50 µL per reaction. Five-microliter samples were amplified for 20, 25, 30, and 35 cycles. DNA quantifications were performed for nonsaturating conditions using Adobe Photoshop software. Primers used for RT-PCR are described in Table 2.

In situ hybridization was performed as described previously (Dinny et al., 2004). The *SERK1* and *SERK2* antisense probes were transcribed using SP6 RNA polymerase (Promega) on M13F/M13R PCR fragments amplified from pGEM-T easy containing the *SERK* ORFs in the proper orientation.

Microscopic Phenotyping of Anthers

Flowers of wild-type and double mutants were incubated for 1 h in Alexander's solution (Alexander, 1969) and then cleared in Herr's solution (Herr, 1971) for 2 h. Cross sections were prepared as described for GUS lines. Differential interference contrast pictures were taken from Herr-cleared young buds using an inverted microscope (Nikon TE300) coupled to a digital camera (Nikon D100).

For confocal observation of nuclei, plants were fixed and stained with propidium iodide as described previously (Laufs et al., 1998). Development stages of anthers were defined in accordance with Sanders et al. (1999). Data were acquired using an inverted microscope (Nikon TE2000-U) set up with a QLC100 Dual Nipkow spinning disk (Solamere Technologies), an argon laser (LaserPhysics), and a CCD camera (Photometrics CoolSNAP HQ) controlled by Metamorph software (Universal Imaging). Laser excitation was 488 nm and emission 600 or 510 nm for propidium iodide and autofluorescence background, respectively. The number of microsporocytes was determined using confocal microscopy on propidium iodide-stained stamens at premeiotic stages. Z-stacks with 0.7- to 1-µm intervals were recorded, including whole microsporangia, and used to count the typical microsporocyte nuclei. To avoid a positional artifact between external and internal microsporangia of the same stamen, both were systematically measured.

Accession Numbers

Arabidopsis Genome Initiative numbers for *SERK1*, 2, and 3 are AT1G71830.1, AT1G34210.1, and AT4G33430.1, respectively.

Supplemental Data

The following materials are available in the online version of this article.

Supplemental Text 1. Expression Correlation of *SERK* Genes.

Supplemental Figure 1. *SERK1* and *SERK2* Expression Levels Correlate with Tapetum Markers.

ACKNOWLEDGMENTS

We thank Marty Yanofsky (University of California, San Diego, CA), Sheila McCormick (University of California, Berkeley, CA), and Hong Ma (Pennsylvania State University, University Park, PA) for comments on the manuscript, José Dinny and Brian Crawford (University of California, San Diego, CA) for advice on in situ hybridizations, and Daphné Autran (Institut de Recherche pour le Développement, Montpellier, France) for propidium iodide staining protocols. This work was supported by National Institutes of Health Grant R01GM060396, National Science Foundation Grant MCB 0417118, and in part by Department of Energy Grant DE-FG02-03ER15449 to J.I.S. J.C. was partially supported by a Lavoisier Fellowship from the French Ministry for Sciences and Technologies, and R.R.-P. was supported by a Marie Curie International Fellowship.

Received August 4, 2005; revised October 4, 2005; accepted October 31, 2005; published November 11, 2005.

REFERENCES

- Albrecht, C., Kwaaitaal, M., Hecht, V., Baaijens, E., Kulikova, O., Russinova, E., and de Vries, S.C. (2005). The *Arabidopsis thaliana* SOMATIC EMBRYOGENESIS RECEPTOR-LIKE KINASES1 and 2 control male gametogenesis. *Plant Cell* **17**, 3337–3349.
- Alexander, M.P. (1969). Differential staining of aborted and nonaborted pollen. *Stain Technol.* **44**, 117–122.
- Arizumi, T., Hatakeyama, K., Hinata, K., Inatsugi, R., Nishida, I., Sato, S., Kato, T., Tabata, S., and Toriyama, K. (2004). Disruption of the novel plant protein NEF1 affects lipid accumulation in the plastids of the tapetum and exine formation of pollen, resulting in male sterility in *Arabidopsis thaliana*. *Plant J.* **39**, 170–181.
- Burgess, D.G., Ralston, E.J., Hanson, W.G., Heckert, M., Ho, M., Jenq, T., Palys, J.M., Tang, K., and Gutterson, N. (2002). A novel, two-component system for cell lethality and its use in engineering nuclear male-sterility in plants. *Plant J.* **31**, 113–125.
- Canales, C., Bhatt, A.M., Scott, R., and Dickinson, H. (2002). *EXS*, a putative LRR receptor kinase, regulates male germline cell number and tapetal identity and promotes seed development in *Arabidopsis*. *Curr. Biol.* **12**, 1718–1727.
- Chen, L., and Bush, D.R. (1997). LHT1, a lysine- and histidine-specific amino acid transporter in *Arabidopsis*. *Plant Physiol.* **115**, 1127–1134.
- Chevalier, D., Batoux, M., Fulton, L., Pfister, K., Yadav, R.K., Schellenberg, M., and Schneitz, K. (2005). STRUBBELIG defines a receptor kinase-mediated signaling pathway regulating organ development in *Arabidopsis*. *Proc. Natl. Acad. Sci. USA* **102**, 9074–9079.
- Clough, S.J., and Bent, A.F. (1998). Floral dip: A simplified method for *Agrobacterium*-mediated transformation of *Arabidopsis thaliana*. *Plant J.* **16**, 735–743.
- Diebart, A., Dalal, M., Tax, F.E., Lacey, A.D., Huttly, A., Li, J., and Clark, S.E. (2003). *CLAVATA1* dominant-negative alleles reveal functional overlap between multiple receptor kinases that regulate meristem and organ development. *Plant Cell* **15**, 1198–1211.
- Dinny, J.R., Yadegari, R., Fischer, R.L., Yanofsky, M.F., and Weigel, D. (2004). The role of JAGGED in shaping lateral organs. *Development* **131**, 1101–1110.
- Fletcher, J.C. (2002). Shoot and floral meristem maintenance in *Arabidopsis*. *Annu. Rev. Plant Biol.* **53**, 45–66.

- Fritz-Laylin, L.K., Krishnamurthy, N., Tor, M., Sjolander, K.V., and Jones, J.D. (2005). Phylogenomic analysis of the receptor-like proteins of rice and *Arabidopsis*. *Plant Physiol.* **138**, 611–623.
- Hecht, V., Vielle-Calzada, J.P., Hartog, M.V., Schmidt, E.D., Boutilier, K., Grossniklaus, U., and de Vries, S.C. (2001). The *Arabidopsis* SOMATIC EMBRYOGENESIS RECEPTOR KINASE 1 gene is expressed in developing ovules and embryos and enhances embryogenic competence in culture. *Plant Physiol.* **127**, 803–816.
- Hellens, R.P., Edwards, E.A., Leyland, N.R., Bean, S., and Mullineaux, P.M. (2000). pGreen: A versatile and flexible binary Ti vector for Agrobacterium-mediated plant transformation. *Plant Mol. Biol.* **42**, 819–832.
- Herr, J.M. (1971). A new clearing-squash technique for the study of ovule development in angiosperms. *Am. J. Bot.* **58**, 785–790.
- Ito, T., and Shinozaki, K. (2002). The MALE STERILITY1 gene of *Arabidopsis*, encoding a nuclear protein with a PHD-finger motif, is expressed in tapetal cells and is required for pollen maturation. *Plant Cell Physiol.* **43**, 1285–1292.
- Kinoshita, T., Cano-Delgado, A., Seto, H., Hiranuma, S., Fujioka, S., Yoshida, S., and Chory, J. (2005). Binding of brassinosteroids to the extracellular domain of plant receptor kinase BRI1. *Nature* **433**, 167–171.
- Koltunow, A.M., Truettner, J., Cox, K.H., Wallroth, M., and Goldberg, R.B. (1990). Different temporal and spatial gene expression patterns occur during anther development. *Plant Cell* **2**, 1201–1224.
- Kwaaitaal, M., de Vries, S.C., and Russinova, E. (2005). *Arabidopsis thaliana* Somatic Embryogenesis Receptor Kinase 1 protein is present in sporophytic and gametophytic cells and undergoes endocytosis. *Protoplasma* **226**, 55–65.
- Larkin, J.C., Brown, M.L., and Schiefelbein, J. (2003). How do cells know what they want to be when they grow up? Lessons from epidermal patterning in *Arabidopsis*. *Annu. Rev. Plant Biol.* **54**, 403–430.
- Laufs, P., Grandjean, O., Jonak, C., Kieu, K., and Traas, J. (1998). Cellular parameters of the shoot apical meristem in *Arabidopsis*. *Plant Cell* **10**, 1375–1390.
- Leonhardt, N., Kwak, J.M., Waner, D., Robert, N., Leonhardt, G., and Schroeder, J.I. (2004). Microarray expression analyses of *Arabidopsis* guard cells and isolation of a recessive abscisic acid hypersensitive protein phosphatase 2C mutant. *Plant Cell* **16**, 596–615.
- Li, J., Wen, J., Lease, K.A., Doke, J.T., Tax, F.E., and Walker, J.C. (2002). BAK1, an *Arabidopsis* LRR receptor-like protein kinase, interacts with BRI1 and modulates brassinosteroid signaling. *Cell* **110**, 213–222.
- Ma, H. (2005). Molecular genetic analyses of microsporogenesis and microgametogenesis in flowering plants. *Annu. Rev. Plant Biol.* **56**, 393–434.
- Mariani, C., Beuckeleer, M.D., Truettner, J., Leemans, J., and Goldberg, R.B. (1990). Induction of male sterility in plants by a chimaeric ribonuclease gene. *Nature* **347**, 384–387.
- Nam, K.H., and Li, J. (2002). BRI1/BAK1, a receptor kinase pair mediating brassinosteroid signaling. *Cell* **110**, 203–212.
- Rhee, S.Y., Osborne, E., Poindexter, P.D., and Somerville, C.R. (2003). Microspore separation in the *quartet 3* mutants of *Arabidopsis* is impaired by a defect in a developmentally regulated polygalacturonase required for pollen mother cell wall degradation. *Plant Physiol.* **133**, 1170–1180.
- Rubinelli, P., Hu, Y., and Ma, H. (1998). Identification, sequence analysis and expression studies of novel anther-specific genes of *Arabidopsis thaliana*. *Plant Mol. Biol.* **37**, 607–619.
- Sanders, P.M., Bui, A.Q., Weterings, K., McIntire, K.N., Hsu, Y.C., Lee, P.Y., Truong, M.T., Beals, T.P., and Goldberg, R.B. (1999). Anther developmental defects in *Arabidopsis thaliana* male-sterile mutants. *Sex. Plant Reprod.* **11**, 297–322.
- Schiefthaler, U., Balasubramanian, S., Sieber, P., Chevalier, D., Wisman, E., and Schneitz, K. (1999). Molecular analysis of NOZZLE, a gene involved in pattern formation and early sporogenesis during sex organ development in *Arabidopsis thaliana*. *Proc. Natl. Acad. Sci. USA* **96**, 11664–11669.
- Schmidt, E.D., Guzzo, F., Toonen, M.A., and de Vries, S.C. (1997). A leucine-rich repeat containing receptor-like kinase marks somatic plant cells competent to form embryos. *Development* **124**, 2049–2062.
- Shah, K., Gadella, T.W., Jr., van Erp, H., Hecht, V., and de Vries, S.C. (2001). Subcellular localization and oligomerization of the *Arabidopsis thaliana* Somatic Embryogenesis Receptor Kinase 1 protein. *J. Mol. Biol.* **309**, 641–655.
- Shiu, S.H., and Bleeker, A.B. (2001). Receptor-like kinases from *Arabidopsis* form a monophyletic gene family related to animal receptor kinases. *Proc. Natl. Acad. Sci. USA* **98**, 10763–10768.
- Shpak, E.D., Berthiaume, C.T., Hill, E.J., and Torii, K.U. (2004). Synergistic interaction of three ERECTA-family receptor-like kinases controls *Arabidopsis* organ growth and flower development by promoting cell proliferation. *Development* **131**, 1491–1501.
- Shpak, E.D., Lakeman, M.B., and Torii, K.U. (2003). Dominant-negative receptor uncovers redundancy in the *Arabidopsis* ERECTA leucine-rich repeat receptor-like kinase signaling pathway that regulates organ shape. *Plant Cell* **15**, 1095–1110.
- Shpak, E.D., McAbee, J.M., Pillitteri, L.J., and Torii, K.U. (2005). Stomatal patterning and differentiation by synergistic interactions of receptor kinases. *Science* **309**, 290–293.
- Wang, X., Goshe, M.B., Soderblom, E.J., Phinney, B.S., Kuchar, J.A., Li, J., Asami, T., Yoshida, S., Huber, S.C., and Clouse, S.D. (2005a). Identification and functional analysis of in vivo phosphorylation sites of the *Arabidopsis* BRASSINOSTEROID-INSENSITIVE1 receptor kinase. *Plant Cell* **17**, 1685–1703.
- Wang, X., Li, X., Meisenhelder, J., Hunter, T., Yoshida, S., Asami, T., and Chory, J. (2005b). Autoregulation and homodimerization are involved in the activation of the plant steroid receptor BRI1. *Dev. Cell* **8**, 855–865.
- Weiss, H., and Maluszynska, J. (2001). Molecular cytogenetic analysis of polyploidization in the anther tapetum of diploid and autotetraploid *Arabidopsis thaliana* plants. *Ann. Bot. (Lond.)* **87**, 729–735.
- Wilson, Z.A., Morroll, S.M., Dawson, J., Swarup, R., and Tighe, P.J. (2001). The *Arabidopsis* MALE STERILITY1 (*MS1*) gene is a transcriptional regulator of male gametogenesis, with homology to the PHD-finger family of transcription factors. *Plant J.* **28**, 27–39.
- Yang, S.L., Jiang, L., Puah, C.S., Xie, L.F., Zhang, X.Q., Chen, L.Q., Yang, W.C., and Ye, D. (2005). Overexpression of *TAPETUM DETERMINANT1* alters the cell fates in the *Arabidopsis* carpel and tapetum via genetic interaction with *EXCESS MICROSPOROXYTES1/EXTRA SPOROGENOUS CELLS*. *Plant Physiol.* **139**, 186–191.
- Yang, S.L., Xie, L.F., Mao, H.Z., Puah, C.S., Yang, W.C., Jiang, L., Sundaresan, V., and Ye, D. (2003). *TAPETUM DETERMINANT1* is required for cell specialization in the *Arabidopsis* anther. *Plant Cell* **15**, 2792–2804.
- Yang, W.C., Ye, D., Xu, J., and Sundaresan, V. (1999). The *SPOROXYTELESS* gene of *Arabidopsis* is required for initiation of sporogenesis and encodes a novel nuclear protein. *Genes Dev.* **13**, 2108–2117.
- Zhao, D.Z., Wang, G.F., Speal, B., and Ma, H. (2002). The *EXCESS MICROSPOROXYTES1* gene encodes a putative leucine-rich repeat receptor protein kinase that controls somatic and reproductive cell fates in the *Arabidopsis* anther. *Genes Dev.* **16**, 2021–2031.
- Zimmermann, P., Hirsch-Hoffmann, M., Hennig, L., and Gruissem, W. (2004). GENEVESTIGATOR. *Arabidopsis* microarray database and analysis toolbox. *Plant Physiol.* **136**, 2621–2632.